One-step implementation of a coherent conversion between microwave and optical cavities via an ensemble of nitrogen-vacancy centers

Tong Liu, Jun-Long Zhao, Bao-Qing Guo, Qi-Cheng Wu, Yan-Hui Zhou, and Chui-Ping Yang

Phys. Rev. A **103**, 023706 — Published 9 February 2021

DOI: 10.1103/PhysRevA.103.023706

One-step implementation of a coherent conversion between microwave and optical cavities via an ensemble of NV centers

Tong Liu[1], Jun-Long Zhao[1], Bao-Qing Guo[1], Qi-Cheng Wu[1], Yan-Hui Zhou[1], and Chui-Ping Yang[1,2*]

[1] *Quantum Information Research Center, Shangrao Normal University, Shangrao 334001, China and*

[2] *Department of Physics, Hangzhou Normal University, Hangzhou 311121, China*

Quantum conversion between microwave and optical photons is an important area of quantum information science and technology. Here we propose a one-step method to realize a coherent conversion between a microwave cavity and an optical cavity utilizing a nitrogen-vacancy center ensemble (NV ensemble). An NV ensemble considered here acts as a quantum transducer, dispersively coupled to the microwave and optical cavities, enabling transfer of quantum state and generating entangled states between microwave and optical cavities. With state-of-the-art technology, the numerical simulation is performed to demonstrate that cat states and Fock states can be high-fidelity transferred and a maximally entangled state can be efficiently synthesized between microwave and optical cavities.

I. INTRODUCTION

Quantum conversion is particularly appealing and plays an important role in quantum information science and technology [1–3]. Microwave photons can be effectively generated and manipulated, while optical photons can be coherently transmitted by optical fibers enabling long distance quantum communication and quantum information processing (QIP). The reversible conversion between microwave and optical photons will connect microwave and optical domains, which makes it suitable for the realization of large-scale quantum networks over a long distance.

A quantum transducer is a necessary requirement for an efficient conversion between microwave and optical photons. In recent years, several theoretical proposals for a transducer have been proposed using various physical systems, including optomechanical systems [4–7], NV centers [8, 9], atoms [10–12], electro-optical systems [13, 14], magnons [16], rare-earth-doped crystals [17, 18], superconducting circuits [19], and solid-state spins [20]. Recently, the coherent conversion between microwave and optical photons has been demonstrated experimentally in optomechanical systems [21, 22], electro-optical systems [23], atoms [24], and rare-earth-doped crystals [25].

An ensemble of NV centers has been considered as a good quantum memory element in QIP [26]. Up to now, a lifetime of 1 s for an NV ensemble has been experimentally reported [27]. Based on NV ensembles, a number of quantum operations such as information transfer, entanglement preparation, and quantum gates have been investigated both in theory [28–39] and experiment [40–43]. Moreover, an NV ensemble is one of the most promising candidates for a microwave-to-optical transducer due to the fact that it can strongly couple to both microwave and optical cavities. So far, the strong coupling of NV centers to superconducting [44–47] and optical [48–51] cavities have been experimentally realized, respectively.

In this paper, we present that an ensemble of NV centers can enable the coherent conversion and especially the transfer of quantum states as well as the generation of entangled states between microwave and optical cavities. The NV ensemble acts as a quantum transducer, which is dispersively coupled to microwave and optical cavities. This proposal has the following features and advantages: (i) The coherent microwave-optical conversion of photons can be implemented using a single-step operation. (ii) Because the NV ensemble is unexcited during the entire process, decoherence from the NV ensemble is greatly suppressed. (iii) This proposal allows the efficient transfer of a discrete-variable or continuous-variable state between microwave and optical cavities. (iv) The proposal can be applied to other physical systems such as microwave and optical cavities coupled to a single atom or an atomic ensemble.

The structure of this paper is as follows. In Sec. II, we introduce our hybrid system and show how to realize a coherent coupling between microwave and optical cavities. In Sec. III, we show how to use the coherent coupling Hamiltonian to transfer quantum states and create maximally entangled states between microwave and optical cavities. In Sec. IV, we discuss the possible experimental implementation of our proposal and numerically calculate the operational fidelity for transferring cat states and Fock states and generating a maximally entangled state of the microwave and optical cavities. A brief concluding summary is given in Sec. V.

II. MODEL AND HAMILTONIAN

Consider a hybrid system consisting of a planar microwave cavity and an optical cavity coupled to an ensemble of NV centers [Fig. 1(a)]. The energy-level of an NV center consists of a ground state ^3A, an excited state ^3E and a metastable state ^1A. Both ^3A and ^3E are spin triplet states while the metastable ^1A

* yangcp@hznu.edu.cn

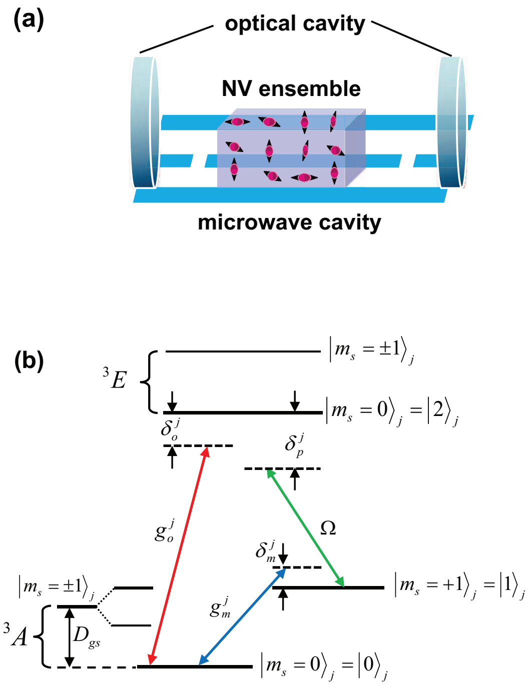

FIG. 1. (color online) (a) Schematic diagram of a hybrid setup for a planar microwave cavity and an optical cavity being coupled to an ensemble of NV centers. (b) Schematic diagram of the energy level splittings of a sing NV center j. Microwave (optical) cavity is far-off resonant with the $|0\rangle_j \leftrightarrow |1\rangle_j$ ($|0\rangle_j \leftrightarrow |2\rangle_j$) transition of NV center j with coupling strength g_m^j (g_o^j) and detuning δ_m^j (δ_o^j), laser pulse is far-off resonant with the $|1\rangle_j \leftrightarrow |2\rangle_j$ transition of NV center j with Rabi frequency Ω and detuning δ_p^j. D_{gs} is the zero-field splitting between the levels $|m_s = 0\rangle_j$ and $|m_s = \pm 1\rangle_j$. By applying a magnetic field along the crystalline axis, the $|m_s = \pm 1\rangle_j$ further split into $|m_s = +1\rangle_j$ and $|m_s = -1\rangle_j$. We choose a subspace $\{|^3A, m_s = 0\rangle_j, |^3A, m_s = +1\rangle_j, |^3E, m_s = 0\rangle_j\}$ as the three logical states $\{|0\rangle_j, |1\rangle_j, |2\rangle_j\}$ of NV center j.

is a spin singlet state [52, 53]. The NV center has an electronic spin triplet ground state with zero-field splitting $D_{gs}/(2\pi) \approx 2.878$ GHz between the $|m_s = 0\rangle$ and $|m_s = \pm 1\rangle$ levels. By applying an external magnetic field along the crystalline axis of the NV center [54, 55], an additional Zeeman splitting between $|m_s = \pm 1\rangle$ sublevels occurs, as illustrated in Fig. 1(b).

An NV center is usually treated as a spin while an ensemble of NV centers is treated as a spin ensemble. As shown in Fig. 1(b), microwave and optical cavity are off-resonantly coupled to an NV ensemble. Here, we choose the microwave cavity is coupled to the transition between the ground level $|^3A, m_s = 0\rangle_j$ and the first excited level $|^3A, m_s = +1\rangle_j$ of the spins in the ensemble, while the optical cavity is coupled to the transition between the ground level $|^3A, m_s = 0\rangle_j$ and the second excited level $|^3E, m_s = 0\rangle_j$ of the spins in the ensemble ($j = 1, 2, 3, \cdots, N$). In addition, a laser pulse is coupled to the $|^3A, m_s = +1\rangle_j \leftrightarrow |^3E, m_s = 0\rangle_j$ transition of the spins. For simplicity, we label the ground state $|^3A, m_s = 0\rangle_j$, the first excited state $|^3A, m_s = +1\rangle_j$ and the second excited state $|^3E, m_s = 0\rangle_j$ of spin j in the ensemble as $|0\rangle_j$, $|1\rangle_j$, and $|2\rangle_j$. We introduce coupling strengths $g_m = \sqrt{\sum_{j=1}^N |g_m^j|^2/N}$ and $g_o = \sqrt{\sum_{j=1}^N |g_o^j|^2/N}$ to denote the average coupling strengths for each spin of the ensemble, where g_m^j (g_o^j) is the coupling strength of the microwave cavity (optical cavity) with the $|0\rangle_j \leftrightarrow |1\rangle_j$ ($|0\rangle_j \leftrightarrow |2\rangle_j$) transition of the jth spin for the ensemble. Moreover, we assume that the NV centers in the ensemble are sufficiently far apart so that the direct spin-spin interactions can be ignored [56]. Typically, the NV-NV coupling strength is within a range of few kHz to tens of kHz when the distance between NV centers is within 20 nm [57]. Recently, Ref. [58] has reported that the effect of the direct NV-NV interactions on the dynamics of a microwave cavity-NV ensemble (with the number of 10^{12} NV spins) system is negligible, and Ref. [59] has demonstrated that the direct NV-NV interactions can be safely ignored for an average NV-NV distance of 60 nm.

In the interaction picture, after making the rotating-wave approximation, the Hamiltonian of the cavities and the NV ensemble is (in units of $\hbar = 1$)

$$\begin{aligned} H_I = & \sum_{j=1}^N g_m (a^\dagger \tau_{10}^{j-} e^{-i\delta_m^j t} + a \tau_{10}^{j+} e^{i\delta_m^j t}) \\ & + \sum_{j=1}^N g_o (b^\dagger \tau_{20}^{j-} e^{-i\delta_o^j t} + b \tau_{20}^{j+} e^{i\delta_o^j t}) \\ & + \sum_{j=1}^N \Omega (\tau_{21}^{j+} e^{i\delta_p^j t} + \tau_{21}^{j-} e^{-i\delta_p^j t}), \end{aligned} \tag{1}$$

where a and $a^\dagger$ (b and $b^\dagger$) are the annihilation and creation operators for the microwave (optical) cavity, $\tau_{10}^{j-} = |0\rangle_j\langle 1|$, $\tau_{10}^{j+} = |1\rangle_j\langle 0|$, $\tau_{20}^{j-} = |0\rangle_j\langle 2|$, $\tau_{20}^{j+} = |2\rangle_j\langle 0|$, $\tau_{21}^{j-} = |1\rangle_j\langle 2|$, and $\tau_{21}^{j+} = |2\rangle_j\langle 1|$ are the lowering and raising operators of the jth spin for the ensemble, $\delta_m^j = \omega_{10}^j - \omega_m$, $\delta_o^j = \omega_{20}^j - \omega_o$, and $\delta_p^j = \omega_{21}^j - \omega_p$ are the detunings, Ω is the Rabi frequency of the laser pulse. Here, ω_{10}^j, ω_{21}^j, and ω_{20}^j are the $|0\rangle_j \leftrightarrow |1\rangle_j$, $|1\rangle_j \leftrightarrow |2\rangle_j$, and $|0\rangle_j \leftrightarrow |2\rangle_j$ transition frequencies of the jth spin for the ensemble, respectively. While ω_m, ω_o, and ω_p are the frequencies of the microwave cavity, optical cavity, and laser pulse, respectively. Because random distributions of spins in the diamond may lead to an inhomogeneous broadening of spin transition for a spin ensemble, we consider random shifts $\Delta_m^j = \delta_m^j - \delta_m$, $\Delta_o^j = \delta_o^j - \delta_o$ and $\Delta_p^j = \delta_p^j - \delta_p$ for the jth spin of the ensemble [9, 34, 38]. Here, δ_m, δ_o and δ_p are the average detunings.

Applying the large-detuning conditions $|\delta_o| \gg \{g_o, |\Delta_o^j|\}$ and $|\delta_p| \gg \{\Omega, |\Delta_p^j|\}$, one can ignore the effect of inhomogeneous broadening for the transition frequencies of the spin ensemble in the following [9, 34, 38]. Moreover, under the conditions

$$|\delta_o - \delta_m| \gg \frac{g_o g_m}{2}\left(\frac{1}{\delta_o} + \frac{1}{\delta_m}\right) \text{ and}$$
$$|\delta_p - \delta_m| \gg \frac{\Omega g_m}{2}\left(\frac{1}{\delta_p} + \frac{1}{\delta_m}\right), \tag{2}$$

the Hamiltonian (1) becomes [60, 61]

$$\begin{aligned} H_e = &\sum_{j=1}^{N} \frac{{g_o}^2}{\delta_o}\left(bb^\dagger|2\rangle_j\langle 2| - b^\dagger b|0\rangle_j\langle 0|\right) \\ &+ \sum_{j=1}^{N} \frac{\Omega^2}{\delta_p}\left(|2\rangle_j\langle 2| - |1\rangle_j\langle 1|\right) \\ &- \sum_{j=1}^{N} \lambda_{op}(b^\dagger \tau_{10}^{j-} e^{-i\delta_{op}t} + b\tau_{10}^{j+} e^{i\delta_{op}t}) \\ &+ \sum_{j=1}^{N} g_m(a^\dagger \tau_{10}^{j-} e^{-i\delta_m t} + a\tau_{10}^{j+} e^{i\delta_m t}), \end{aligned} \tag{3}$$

where $\lambda_{op} = \frac{g_o\Omega}{2}(\frac{1}{\delta_o} + \frac{1}{\delta_p})$ and $\delta_{op} = \delta_o - \delta_p$. Note that the first and second lines of Eq. (3) describe Stark shifts, the third line of Eq. (3) represents the effective coupling between the $|0\rangle_j \leftrightarrow |1\rangle_j$ transition of the jth spin and the optical cavity.

Under the conditions of the weak excitations and the large N, we can map the spin operators to the bosonic operators by using the Holstein-Primakoff transformation [62, 63]: $\sum_{j=1}^{N}\tau_{10}^{j-} \simeq \sqrt{N}c$, $\sum_{j=1}^{N}\tau_{10}^{j+} \simeq \sqrt{N}c^\dagger$, and $\sum_{j=1}^{N}\tau_z^j = 2c^\dagger c - N$, where the operators c and $c^\dagger$ behaves as bosonic operators and the spin ensemble behaves as a bosonic mode. Thus, one has $[c, c^\dagger] \approx 1$ and $\sum_{j=1}^{N}|0\rangle_j\langle 0| = \sum_{j=1}^{N}\frac{1}{2}(\mathbb{I}_j - \tau_z^j) = N - c^\dagger c$.

When each spin is in the ground state, the first term in the first bracket of the first line and all terms in the second line of Eq. (3) can be eliminated. Therefore, Eq. (3) can be further rewritten as

$$\begin{aligned} H_e = &-\frac{Ng_o^2}{\delta_o}b^\dagger b + \frac{g_o^2}{\delta_o}b^\dagger bc^\dagger c \\ &- G_1(b^\dagger ce^{-i\delta_{op}t} + bc^\dagger e^{i\delta_{op}t}) \\ &+ G_2(a^\dagger ce^{-i\delta_m t} + ac^\dagger e^{i\delta_m t}), \end{aligned} \tag{4}$$

where $G_1 = \frac{\sqrt{N}g_o\Omega}{2}(\frac{1}{\delta_o} + \frac{1}{\delta_p})$ and $G_2 = \sqrt{N}g_m$.

Applying the large-detuning conditions $|\delta_{op}| \gg G_1$ and $|\delta_m| \gg \{G_2, |\Delta_m^j|\}$, the Hamiltonian (4) becomes [60, 61]

$$H_e = H_0 + H_i \tag{5}$$

with

$$\begin{aligned} H_0 &= -\frac{G_2^2}{\delta_m}a^\dagger a - \left(\frac{Ng_o^2}{\delta_o} + \frac{G_1^2}{\delta_{op}}\right)b^\dagger b, \\ H_i &= \lambda\left[a^\dagger be^{i(\delta_{op}-\delta_m)t} + b^\dagger ae^{-i(\delta_{op}-\delta_m)t}\right], \end{aligned} \tag{6}$$

where $\lambda = \frac{G_1G_2}{2}(\frac{1}{\delta_{op}} + \frac{1}{\delta_m})$ and we have used $[c, c^\dagger] = 1$ and $c^\dagger c|0\rangle_c = 0$. The Hamiltonian H_0 describes Stark shifts, where the degree of freedom for the spin ensemble has been omitted because the spin ensemble is in the ground state $|0\rangle_c$. The Hamiltonian H_i shows the effective coupling between the microwave cavity and the optical cavity with the effective coupling strength λ.

In a new interaction picture with respect to the Hamiltonian H_0, one obtains

$$\begin{aligned} H_e &= e^{iH_0t}H_ie^{-iH_0t} \\ &= \lambda\left[e^{i(\frac{Ng_o^2}{\delta_o} + \frac{G_1^2}{\delta_{op}} - \frac{G_2^2}{\delta_m})t}e^{i(\delta_{op}-\delta_m)t}a^\dagger b + h.c.\right]. \end{aligned} \tag{7}$$

We have set

$$\frac{Ng_o^2}{\delta_o} + \frac{G_1^2}{\delta_{op}} - \frac{G_2^2}{\delta_m} = -(\delta_{op} - \delta_m), \tag{8}$$

the Hamiltonian (7) thus becomes

$$H_e = \lambda(a^\dagger b + b^\dagger a). \tag{9}$$

The Hamiltonian (9) is the well-known Jaynes-Cummings Hamiltonian, which describes the coherent conversion between a microwave-cavity mode and an optical-cavity mode. In the next section, we first show how to use the effective Hamiltonian (9) to transfer quantum states between the microwave and optical cavities, and then discuss how to use the effective Hamiltonian (9) to create a maximally entangled state of the microwave and optical cavities.

III. QUANTUM STATE TRANSFER AND ENTANGLEMENT BETWEEN MICROWAVE AND OPTICAL CAVITIES

Now we show that the effective Hamiltonian (9) can be used to transfer quantum states between the microwave and optical cavities. From Eq. (9), the Heisenberg equations for the operators $a^\dagger$ and $b^\dagger$ are

$$\begin{aligned} \dot{a^\dagger} &= i\lambda b^\dagger, \\ \dot{b^\dagger} &= i\lambda a^\dagger. \end{aligned} \tag{10}$$

The solution of Eq. (10) is given by

$$\begin{aligned} a^\dagger(t) &= \cos(\lambda t)\, a^\dagger + i\sin(\lambda t)\, b^\dagger, \\ b^\dagger(t) &= \cos(\lambda t)\, b^\dagger + i\sin(\lambda t)\, a^\dagger. \end{aligned} \tag{11}$$

According to Eq. (11), one has $a^\dagger(t) = ib^\dagger$ and $b^\dagger(t) = ia^\dagger$ for $t = \pm\pi/(2\lambda)$. Here, the sign " + " or " − " depends on the detuning δ_{op} $(\delta_m) > 0$ or δ_{op} $(\delta_m) < 0$.

We suppose that the microwave cavity is initially in an arbitrary pure state $|\psi\rangle_a = \sum_{n=0}^{\infty} c_n|n\rangle_a$, while the optical cavity is initially in an arbitrary pure state $|\varphi\rangle_b = \sum_{m=0}^{\infty} d_m|m\rangle_b$. Here, $|n\rangle_a = \frac{(a^\dagger)^n}{\sqrt{n!}}|0\rangle_a$ and $|m\rangle_b = \frac{(b^\dagger)^m}{\sqrt{m!}}|0\rangle_b$. With the effective Hamiltonian (9) and after the evolution time $t = \pi/(2|\lambda|)$, the state $|\psi\rangle_a|\varphi\rangle_b$ of the cavity-system evolves into [64]

$$\begin{aligned}
& e^{-iH_e t}|\psi\rangle_a|\varphi\rangle_b \\
&= \sum_{n=0}^{\infty}\sum_{m=0}^{\infty} \frac{c_n}{\sqrt{n!}}\frac{d_m}{\sqrt{m!}} e^{-iH_e t}(a^\dagger)^n(b^\dagger)^m|0\rangle_a|0\rangle_b \\
&= \sum_{n=0}^{\infty}\sum_{m=0}^{\infty} \frac{c_n}{\sqrt{n!}}\frac{d_m}{\sqrt{m!}} \left[e^{iH_e t}(a^\dagger)^n e^{-iH_e t}\right] \\
&\otimes \left[e^{iH_e t}(b^\dagger)^m e^{-iH_e t}\right] e^{iH_e t}|0\rangle_a|0\rangle_b \\
&= \sum_{m=0}^{\infty} \frac{d_m}{\sqrt{m!}}(ia^\dagger)^m|0\rangle_a \sum_{n=0}^{\infty} \frac{c_n}{\sqrt{n!}}(ib^\dagger)^n|0\rangle_b \\
&= \sum_{m=0}^{\infty} e^{i\frac{\pi}{2}m} d_m|m\rangle_a \sum_{n=0}^{\infty} e^{i\frac{\pi}{2}n} c_n|n\rangle_b \\
&= |\varphi\rangle_a|\psi\rangle_b,
\end{aligned} \tag{12}$$

where we have used $a|0\rangle_a = 0$, $b|0\rangle_b = 0$, $(i)^m = e^{i\frac{\pi}{2}m}$, and $(i)^n = e^{i\frac{\pi}{2}n}$, and we have dropped the phase shifts $e^{i\frac{\pi}{2}n}$ and $e^{i\frac{\pi}{2}m}$, which can be corrected by the local rotations. Eq. (12) shows that the states of the microwave and the optical cavities are exchanged with each other. Here, the $|\psi\rangle$ and $|\varphi\rangle$ states can be discrete-variable states (e.g., single photon state) or continuous-variable states (e.g., cat state). Microwave photons can be effectively generated and manipulated, while optical photons can be coherently transmitted by optical fibers. Thus, according to Eq. (12), one can transfer an arbitrary state of a microwave cavity to an optical cavity, and then transfer it into a network via optical fibers, which is useful in quantum communication and QIP performed in a large-scale quantum network over a long distance.

The effective Hamiltonian (9) can also be used to generate entangled states of the the microwave and optical cavities. At the evolution time $t = \pi/(4|\lambda|)$, the initial state $|1\rangle_a|0\rangle_b$ of the microwave and optical cavities turns into

$$\frac{1}{\sqrt{2}}(|1\rangle_a|0\rangle_b - i|0\rangle_a|1\rangle_b), \tag{13}$$

which shows that a maximally entangled state between the optical and microwave cavities is created.

IV. POSSIBLE EXPERIMENTAL IMPLEMENTATION

After taking into account the dissipation and the dephasing of the cavities and the NV ensemble, the dynamics of the lossy system is governed by the Markovian master equation

$$\frac{d\rho}{dt} = -i[H_e, \rho] + \kappa_a\mathcal{D}[a] + \kappa_b\mathcal{D}[b] + \kappa_c\mathcal{D}[c], \tag{14}$$

where ρ is the density matrix of the whole system, H_e is given by Eq. (4), $\mathcal{D}[\mathcal{O}] = (2\mathcal{O}\rho\mathcal{O}^+ - \mathcal{O}^+\mathcal{O}\rho - \rho\mathcal{O}^+\mathcal{O})/2$ is the dissipator. In addition, κ_a, κ_b, and κ_c are the decay rates of the microwave cavity, the optical cavity, and the NV ensemble, respectively.

The operation efficiency can be evaluated by fidelity $\mathcal{F} = \sqrt{\langle\psi_{\rm id}|\,\rho\,|\psi_{\rm id}\rangle}$, where $|\psi_{\rm id}\rangle$ is the ideal target state. For an experimental implementation, we consider the NV ensemble is initially in the vacuum state $|0\rangle_c$. The cavity-system initially state $|\psi\rangle_a|\varphi\rangle_b$ is (i) $|\psi_{cat}\rangle_a|0\rangle_b$ and (ii) $|n\rangle_a|0\rangle_b$ for the state transfer, and (iii) $|1\rangle_a|0\rangle_b$ for the generation of the entangled state. Accordingly, the ideal target state is given by (i) $|0\rangle_a|\psi_{cat}\rangle_b$ and (ii) $|0\rangle_a|n\rangle_b$ for the state transfer, and (iii) $\frac{1}{\sqrt{2}}(|1\rangle_a|0\rangle_b - i|0\rangle_a|1\rangle_b)$ for the generation of the entangled state. Here, $|n\rangle$ and $|\psi_{cat}\rangle = N_c(|\alpha\rangle + |-\alpha\rangle)$ with $N_c = \frac{1}{\sqrt{2}}[1+\exp(-2\alpha^2)]^{-1/2}$ are the Fock state and the cat state of the microwave cavity or optical cavity, respectively. Up to now, Fock states [65] or cat states [66] of a microwave cavity have been generated in experiments. Moreover, cat-state qubits can be used in quantum error correction [67], quantum computation [68], and continuous-variable quantum communication [69], etc.

By solving the master equation (14), the fidelity of the state transfer can be calculated for (i) $|\psi_{cat}\rangle_a|0\rangle_b$ and (ii) $|n\rangle_a|0\rangle_b$, respectively. We choose NV ensemble-microwave cavity and NV ensemble-optical cavity coupling constants $\sqrt{N}g_m/2\pi = 11$ MHz and $\sqrt{N}g_o/2\pi = 300$ MHz with the number of NV centers $N \sim 10^{12}$ [44–47], respectively. The values of $\sqrt{N}g_m$ and $\sqrt{N}g_o$ here are available in experiments because the coupling strength $3-65$ MHz between an NV ensemble and a superconducting coplanar waveguide resonator [44–47] and the coupling strength $0.3-1$ GHz between an NV ensemble and an optical cavity [48–51] have been reported in experiments. We assume the inhomogeneous broadening of the transition frequencies for $\Delta_p^j/2\pi = 500$ MHz, $\Delta_o^j/2\pi = 1$ GHz [70] and $\Delta_m^j/2\pi = 10$ MHz [34], which can be achieved with experimentally observed values of $\Delta_o^j/2\pi = 0.45-20$ GHz [71–73] and $\Delta_m^j/2\pi = 6-12$ MHz [58, 74, 75]. In addition, we set $\alpha = 1$, $\Omega/2\pi = 110$ MHz (attainable in experiments [76, 77]), $\kappa_a^{-1} = 15\kappa^{-1}$, $\kappa_b^{-1} = 2\kappa^{-1}$, and $\kappa_c^{-1} = \kappa^{-1}$.

Figure 2 shows the fidelity $\mathcal{F}$ versus $\delta_o/(\sqrt{N}g_o)$ and δ_p/Ω for the transfer of cat state $|\psi_{cat}\rangle_a$, which is plotted by setting $\kappa^{-1} = 1$ μs. The lifetimes of the cavities and the NV ensemble are $\kappa_a^{-1} = 15$ μs, $\kappa_b^{-1} = 2$ μs, and

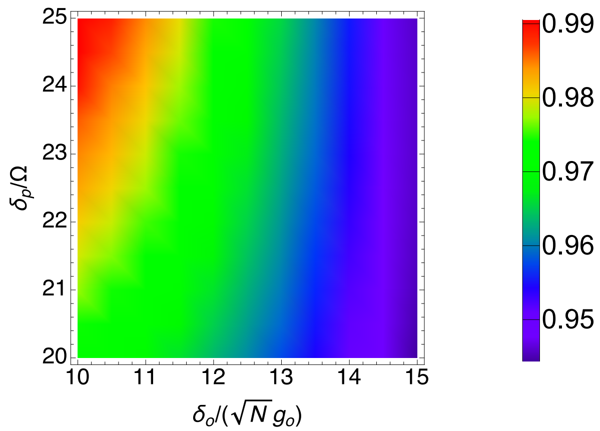

FIG. 2. (color online) Fidelity $\mathcal{F}$ versus $\delta_o/(\sqrt{N}g_o)$ and δ_p/Ω, which is plotted by choosing $\kappa^{-1} = 1\ \mu s$.

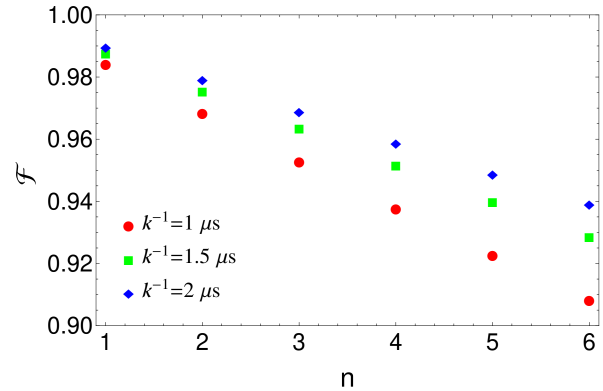

FIG. 3. (color online) Fidelity $\mathcal{F}$ versus the photon number n, which is plotted by choosing (i) $\kappa^{-1} = 1\ \mu s$, (ii) $\kappa^{-1} = 1.5\ \mu s$, and (iii) $\kappa^{-1} = 2\ \mu s$.

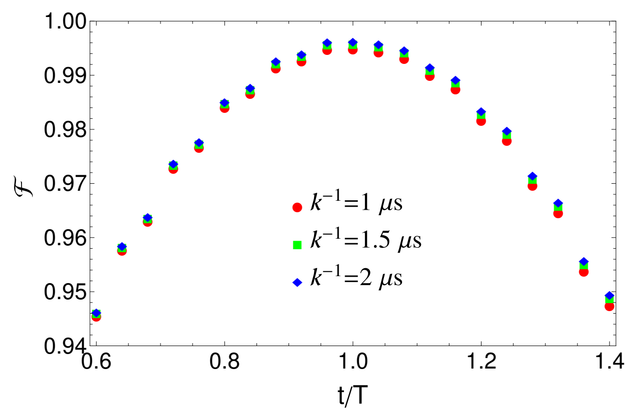

FIG. 4. (color online) Fidelity $\mathcal{F}$ versus t/T, which is plotted by choosing $\kappa^{-1} = 1\ \mu s$, $1.5\ \mu s$, $2\ \mu s$.

$\kappa_c^{-1} = 1\ \mu s$, respectively. Here we consider a rather conservative case for the lifetime of the NV ensemble [78]. For an NV ensemble, the decoherence time$\sim 1\ s$ [27] by using dynamical decoupling techniques and longer than 300 μs [82] have been experimentally reported. For optical and microwave cavities, the lifetimes of 0.1-2.5 ms for optical cavities [79, 80] and 0.3 ms for microwave cavities [81] have been experimentally demonstrated. From Fig. 2, one can see that a high fidelity$\sim$ 99.0% is achievable for $\delta_o/(\sqrt{N}g_o) = 10$ and $\delta_p/\Omega = 25$. For $\delta_o/(\sqrt{N}g_o) = 10$ and $\delta_p/\Omega = 25$, one has detunings $\delta_o/2\pi = 3.0$ GHz and $\delta_p/2\pi = 2.75$ GHz. According to $\delta_m = \delta_o - \delta_p$, one can obtain $\delta_m/2\pi = 0.25$ GHz. Moreover, one has $\delta_p^j/2\pi = 3.25$ GHz, $\delta_o^j/2\pi = 4.0$ GHz, and $\delta_m^j/2\pi = 0.26$ GHz. With the above given parameters, we obtain the effective coupling strength $\lambda/2\pi \sim 0.51$ MHz between the microwave and optical cavities. Thus, the operational time is estimated as 0.5 μs. In Fig. 3 and Fig. 4, we set $\delta_o/(\sqrt{N}g_o) = 10$ and $\delta_p/\Omega = 25$.

Figure 3 displays the fidelity $\mathcal{F}$ versus the photon number n for the transfer of the Fock state $|n\rangle_a$, which is plotted by choosing (i) $\kappa^{-1} = 1\ \mu s$, (ii) $\kappa^{-1} = 1.5\ \mu s$, and (iii) $\kappa^{-1} = 2\ \mu s$. Figure 3 shows that for $n = 1, 2, 3, 4, 5, 6$, the fidelities are approximately (i) 98.41%, 96.83%, 95.28%, 93.76%, 92.27%, and 90.82% for $\kappa^{-1} = 1\ \mu s$, (ii) 98.77%, 97.55%, 96.35%, 95.16%, 94.00%, and 92.86% for $\kappa^{-1} = 1.5\ \mu s$, and (iii) 98.95%, 97.91%, 96.88%, 95.87%, 94.87%, and 93.90% for $\kappa^{-1} = 2\ \mu s$, respectively. These results indicate high fidelities can be obtained for the Fock state transfer with $n \leq 6$. To obtain a high transfer fidelity in the case of large n, our protocol requires a longer lifetime κ^{-1} in the numerical simulation.

We now numerically calculate the fidelity for generation of a maximally entangled state between the microwave and optical cavities. Figure 4 shows the fidelity $\mathcal{F}$ versus t/T for generation of the entangled state by choosing $\kappa^{-1} = 1\ \mu s$, $1.5\ \mu s$, $2\ \mu s$. Here, t is the state evolution time and T is the entire operation time required for the entangled state preparation. For $\delta_o/(\sqrt{N}g_o) = 10$ and $\delta_p/\Omega = 25$, one can obtain the optimal operation time $T \sim 0.25\ \mu s$. Figure 4 displays the optimal fidelities are approximately 99.49%, 99.58%, 99.63% for $\kappa^{-1} = 1\ \mu s$, $1.5\ \mu s$, $2 \mu s$, respectively. Moreover, Fig. 4 shows that for $t/T \in [0.6, 1.4]$, the fidelities are respectively greater than 94.55%, 94.60%, 94.62% for $\kappa^{-1} = 1\ \mu s$, $1.5\ \mu s$, $2\ \mu s$. Thus, the entangled state can be high fidelity generated for small operation time errors.

The simulations above indicate that the high-fidelity transfer of quantum states or the high fidelity generation of a maximally entangled state of the microwave and optical cavities is feasible with present-day experimental technology.

We should mention that the inhomogeneous broadening of an NV ensemble may limit the long spin-dephasing time (T_2^*) and the spin-coherence time (T_2). However, T_2^* and T_2 can be enhanced by suppressing impurities and defects [82], depleting the ^{13}C isotope [83], or using spin-echo techniques [47]. The long spin-coherence time T_2^* (T_2) can be made to be on the order of $0.47 - 1.5$ ms ($0.1 - 2.4$ ms) by the state-of-the-art technology [47, 83, 84]. Alternatively, our proposal can be applied to other emitters with a small inhomogeneous broadening but potentially shorter spin coherence, such as silicon vacancy (SiV) centers in diamond [85–87], SiV in silicon carbide [88, 89], and divacancy in silicon carbide [90, 91].

V. CONCLUSION

We have proposed a method to implementing a coherent conversion between microwave and the optical cavities via an ensemble of NV centers. Due to the NV ensemble dispersively interacting with the microwave cavity and the optical cavity, the effect of cavity decay and the NV ensemble decoherence are greatly suppressed. Because the protocol requires only a single step of operation and employs a three-level of NV ensemble, the operation is simplified and the experimental difficulty is reduced. Our scheme can be used to transfer a discrete-variable or continuous-variable quantum state between microwave and optical cavities. In addition, our method can also be used to create a maximally entangled state of the microwave and optical cavities. Numerical simulation shows that a cat state or a Fock state can be high-fidelity transferred and a maximally entangled state can be high-fidelity generated between the microwave and optical cavities. This work provides a new way for realizing the coherent conversion between microwave and optical cavities, and it may find some applications in quantum information processing.

ACKNOWLEDGEMENTS

This work was partly supported by the Key-Area Research and Development Program of GuangDong Province (2018B030326001), the National Natural Science Foundation of China (NSFC) (12004253, 11074062, 11374083, 11774076, 11804228, 11965017), the NKRDP of China (2016YFA0301802), the Jiangxi Natural Science Foundation (20192ACBL20051), and the Jiangxi Education Department Fund (GJJ190893, GJJ180873).

[1] L. Tian, Optoelectromechanical transducer: Reversible conversion between microwave and optical photons, Annalen Der Physik **527**, 1 (2015).

[2] N. Lauk, N. Sinclair, S. Barzanjeh, J. P. Covey, M. Saffman, M. Spiropulu, and C. Simon, Perspectives on quantum transduction, Quantum Sci. Technol. **5**, 020501 (2020).

[3] N. J. Lambert, A. Rueda, F. Sedlmeir, and H. G. L. Schwefel, Coherent conversion between microwave and optical photonsAn overview of physical implementations, Adv. Quantum Technol. **3**, 1900077 (2020).

[4] K. Stannigel, P. Rabl, A. S. Sørensen, P. Zoller, and M. D. Lukin, Optomechanical transducers for long-distance quantum communication, Phys. Rev. Lett. **105**, 220501 (2010).

[5] S. Barzanjeh, M. Abdi, G. J. Milburn, P. Tombesi, and D. Vitali, Reversible optical-to-microwave quantum interface, Phys. Rev. Lett. **109**, 130503 (2012).

[6] Y. D. Wang and A. A. Clerk, Using interference for high fidelity quantum state transfer in optomechanics, Phys. Rev. Lett. **108**, 153603 (2012).

[7] L. Tian, Adiabatic state conversion and pulse transmission in optomechanical systems, Phys. Rev. Lett. **108**, 153604 (2012).

[8] I. Lekavicius, D. Andrew Golter, T. Oo, and H. Wang, Transfer of phase information between microwave and optical fields via an electron spin, Phys. Rev. Lett. **119**, 063601 (2017).

[9] B. Li, P. B. Li, Y. Zhou, S. L. Ma, and F. L. Li, Quantum microwave-optical interface with nitrogen-vacancy centers in diamond, Phys. Rev. A **96**, 032342 (2017).

[10] M. Hafezi, Z. Kim, S. L. Rolston, L. A. Orozco, B. L. Lev, and J. M. Taylor, Atomic interface between microwave and optical photons, Phys. Rev. A **85**, 020302(R) (2012).

[11] M. Kiffner, A. Feizpour, K. T. Kaczmarek, D. Jaksch, and J. Nunn, Two-way interconversion of millimeter-wave and optical fields in Rydberg gases, New J. Phys. **18**, 093030 (2016).

[12] B. T. Gard, K. Jacobs, R. McDermott, and M. Saffman, Microwave-to-optical frequency conversion using a cesium atom coupled to a superconducting resonator, Phys. Rev. A **96**, 013833 (2017).

[13] M. Tsang, Cavity quantum electro-optics, Phys. Rev. A **81**, 063837 (2010).

[14] M. Soltani, M. Zhang, C. Ryan, G. J. Ribeill, C. Wang, and M. Loncar, Efficient quantum microwave-to-optical conversion using electro-optic nanophotonic coupled resonators, Phys. Rev. A **96**, 043808 (2017).

[15] C. H. Li and P. B. Li, Coupling a single nitrogen-vacancy center with a superconducting qubit via the electro-optic effect, Phys. Rev. A **97**, 052319 (2018).

[16] R. Hisatomi, A. Osada, Y. Tabuchi, T. Ishikawa, A. Noguchi, R. Yamazaki, K. Usami, and Y. Nakamura, Bidirectional conversion between microwave and light via ferromagnetic magnons, Phys. Rev. B **93**, 174427 (2016).

[17] L. A. Williamson, Y. H. Chen, and J. J. Longdell, Magneto-optic modulator with unit quantum efficiency, Phys. Rev. Lett. **113**, 203601 (2014).

[18] C. O'Brien, N. Lauk, S. Blum, G. Morigi, and M. Fleischhauer, Interfacing superconducting qubits and telecom photons via a rare-earth-doped crystal, Phys. Rev. Lett. **113**, 063603 (2014).

[19] C. Zhong, Z. Wang, C. Zou, M. Zhang, X. Han, W. Fu, M. Xu, S. Shankar, M. H. Devoret, H. X. Tang, and L. Jiang, Proposal for heralded generation and detection of entangled microwave-optical-photon pairs, Phys. Rev. Lett. **124**, 010511 (2020).

[20] C. Li and P. Cappellaro, Telecom photon interface of solid-state quantum nodes, J. Phys. Commun. **3**, 095016 (2019).

[21] R. W. Andrews, R. W. Peterson, T. P. Purdy, K. Cicak, R. W. Simmonds, C. A. Regal, and K. W. Lehnert, Bidirectional and efficient conversion between microwave and optical light, Nat. Phys. **10**, 321 (2014).

[22] M. Mirhosseini, A. Sipahigil, M. Kalaee, and O. Painter, Superconducting qubit to optical photon transduction, Nature **588**, 599 (2020).

[23] A. P. Higginbotham, P. S. Burns, M. D. Urmey, R. W. Peterson, N. S. Kampel, B. M. Brubaker, G. Smith, K. W. Lehnert, and C. A. Regal, Harnessing electro-optic correlations in an efficient mechanical converter, Nat. Phys. **14**, 1038 (2018).

[24] J. Han, T. Vogt, C. Gross, D. Jaksch, M. Kiffner, and W. Li, Coherent microwave-to-optical conversion via six-wave mixing in Rydberg atoms, Phys. Rev. Lett. **120**, 093201 (2018).

[25] J. G. Bartholomew, J. Rochman, T. Xie, J. M. Kindem, A. Ruskuc, I. Craiciu, M. Lei, and A. Faraon, On-chip coherent microwave-to-optical transduction mediated by ytterbium in YVO_4, Nat. Commun. **11**, 3266 (2020).

[26] C. Simon, M. Afzelius, J. Appel, A. Boyer de la Giroday, S. J. Dewhurst, N. Gisin, C. Y. Hu, F. Jelezko, S. Kröll, J. H. Müller, J. Nunn, E. S. Polzik, J. G. Rarity, H. De Riedmatten, W. Rosenfeld, A. J. Shields, N. Sköld, R. M. Stevenson, R. Thew, I. A. Walmsley, M. C. Weber, H. Weinfurter, J. Wrachtrup, and R. J. Young, Quantum memories, Eur. Phys. J. D **58**, 1 (2010).

[27] N. Bar-Gill, L. M. Pham, A. Jarmola, D. Budker, and R. L. Walsworth, Solid-state electronic spin coherence time approaching one second, Nat. Commun. **4**, 1743 (2013).

[28] J. H. Wesenberg, A. Ardavan, G. A. D. Briggs, J. J. L. Morton, R. J. Schoelkopf, D. I. Schuster, and K. Mølmer, Quantum computing with an electron spin ensemble, Phys. Rev. Lett. **103**, 070502 (2009).

[29] D. Marcos, M. Wubs, J. M. Taylor, R. Aguado, M. D. Lukin, and A. S. Sørensen, Coupling nitrogen-vacancy centers in diamond to superconducting flux qubits, Phys. Rev. Lett. **105**, 210501 (2010).

[30] W. L. Yang, Y. Hu, Z. Q. Yin, Z. J. Deng, and M. Feng, Entanglement of nitrogen-vacancy-center ensembles using transmission line resonators and a superconducting phase qubit, Phys. Rev. A **83**, 022302 (2011).

[31] T. Hümmer, G. M. Reuther, P. Hänggi, and D. Zueco, Nonequilibrium phases in hybrid arrays with flux qubits and nitrogen-vacancy centers, Phys. Rev. A **85**, 052320 (2012).

[32] Z. L. Xiang, X. Y. Lü, T. F. Li, J. Q. You, and F. Nori, Hybrid quantum circuit consisting of a superconducting flux qubit coupled to a spin ensemble and a transmission-line resonator, Phys. Rev. B **87**, 144516 (2013).

[33] X. Y. Lü, Z. L. Xiang, W. Cui, J. Q. You, and F. Nori, Quantum memory using a hybrid circuit with flux qubits and nitrogen-vacancy centers, Phys. Rev. A **88**, 012329 (2013).

[34] L. J. Zou, D. Marcos, S. Diehl, S. Putz, J. Schmiedmayer, J. Majer, and P. Rabl, Implementation of the Dicke lattice model in hybrid quantum system arrays, Phys. Rev. Lett. **113**, 023603 (2014).

[35] T. Liu, Q. P. Su, S. J. Xiong, J. M. Liu, C. P. Yang, and F. Nori, Generation of a macroscopic entangled coherent state using quantum memories in circuit QED, Sci. Rep. **6**, 32004 (2016).

[36] T. Liu, B. Q. Guo, C. S. Yu, and W. N. Zhang, One-step implementation of a hybrid Fredkin gate with quantum memories and single superconducting qubit in circuit QED and its applications, Opt. Express **26**, 4498 (2018).

[37] M. Li and M. Zhang, Robust universal photonic quantum gates operable with imperfect processes involved in diamond nitrogen-vacancy centers inside low-Q single-sided cavities, Opt. Express **26**, 33129 (2018).

[38] W. J. Su, Z. B. Yang, and Z. R. Zhong, Arbitrary control of entanglement between two nitrogen-vacancy-center ensembles coupling to a superconducting-circuit qubit, Phys. Rev. A **97**, 012329 (2018).

[39] S. L. Ma, X. K. Li, J. K. Xie, and F. L. Li, Two-mode squeezed states of two separated nitrogen-vacancy-center ensembles coupled via dissipative photons of superconducting resonators, Phys. Rev. A **99**, 012325 (2019).

[40] E. Togan, Y. Chu, A. S. Trifonov, L. Jiang, J. Maze, L. Childress, M. V. G. Dutt, A. S. Sørensen, P. R. Hemmer, A. S. Zibrov, and M. D. Lukin, Quantum entanglement between an optical photon and a solid-state spin qubit, Nature **466**, 730 (2010).

[41] X. Zhu, S. Saito, A. Kemp, K. Kakuyanagi, S. Karimoto, H. Nakano, W. J. Munro, Y. Tokura, M. S. Everitt, K. Nemoto, M. Kasu, N. Mizuochi, and K. Semba, Coherent coupling of a superconducting flux qubit to an electron spin ensemble in diamond, Nature **478**, 221 (2011).

[42] Y. Kubo, C. Grezes, A. Dewes, T. Umeda, J. Isoya, H. Sumiya, N. Morishita, H. Abe, S. Onoda, T. Ohshima, V. Jacques, A. Dréau, J. F. Roch, I. Diniz, A. Auffeves, D. Vion, D. Esteve, and P. Bertet, Hybrid quantum circuit with a superconducting qubit coupled to a spin ensemble, Phys. Rev. Lett. **107**, 220501 (2011).

[43] S. Saito, X. Zhu, R. Amsüss, Y. Matsuzaki, K. Kakuyanagi, T. Shimo-Oka, N. Mizuochi, K. Nemoto, W. J. Munro, and K. Semba, Towards realizing a quantum memory for a superconducting qubit: Storage and retrieval of quantum states, Phys. Rev. Lett. **111**, 107008 (2013).

[44] Y. Kubo, F. R. Ong, P. Bertet, D. Vion, V. Jacques, D. Zheng, A. Dréau, J. F. Roch, A. Auffeves, F. Jelezko, J. Wrachtrup, M. F. Barthe, P. Bergonzo, and D. Esteve, Strong coupling of a spin ensemble to a superconducting resonator, Phys. Rev. Lett. **105**, 140502 (2010).

[45] D. I. Schuster, A. P. Sears, E. Ginossar, L. DiCarlo, L. Frunzio, J. J. L. Morton, H. Wu, G. A. D. Briggs, B. B. Buckley, D. D. Awschalom, and R. J. Schoelkopf, High-cooperativity coupling of electron-spin ensembles to superconducting cavities, Phys. Rev. Lett. **105**, 140501 (2010).

[46] R. Amsüss, Ch. Koller, T. Nöbauer, S. Putz, S. Rotter, K. Sandner, S. Schneider, M. Schramböck, G. Steinhauser, H. Ritsch, J. Schmiedmayer, and J. Majer, Cavity QED with magnetically coupled collective ppin states, Phys. Rev. Lett. **107**, 060502 (2011).

[47] B. Julsgaard, C. Grezes, P. Bertet, and K. Mølmer, Quantum memory for microwave photons in an inhomogeneously broadened spin ensemble, Phys. Rev. Lett. **110**, 250503 (2013).

[48] Y. S. Park, A. K. Cook, and H. Wang, Cavity QED with diamond nanocrystals and silica microspheres, Nano Lett. **6**, 2075 (2006).

[49] S. Schietinger, T. Schröder, and O. Benson, One-by-one coupling of single defect centers in nanodiamonds to high-

Q modes of an optical microresonator, Nano Lett. **8**, 3911 (2008).
[50] P. E. Barclay, K. M. C. Fu, C. Santori, and R. G. Beausoleil, Chip-based microcavities coupled to nitrogen-vacancy centers in single crystal diamond, Appl. Phys. Lett. **95**, 191115 (2009).
[51] P. E. Barclay, C. Santori, K. M. Fu, R. G. Beausoleil, and O. Painter, Coherent interference effects in a nano-assembled diamond NV center cavity-QED system, Opt. Express **17**, 8081 (2009).
[52] A. Lenef and S. C. Rand, Electronic structure of the N-V center in diamond: Theory, Phys. Rev. B **53**, 13441 (1996).
[53] N. B. Manson, J. P. Harrison, and M. J. Sellars, Nitrogen-vacancy center in diamond: Model of the electronic structure and associated dynamics, Phys. Rev. B **74**, 104303 (2006).
[54] P. Neumann, R. Kolesov, V. Jacques, J. Beck, J. Tisler, A. Batalov, L. Rogers, N. B. Manson, G. Balasubramanian, F. Jelezko, and J. Wrachtrup, Excited-state spectroscopy of single NV defects in diamond using optically detected magnetic resonance, New J. Phys. **11**, 013017 (2009).
[55] W. Yang, Z. Xu, M. Feng, and J. Du, Entanglement of separate nitrogen-vacancy centers coupled to a whispering-gallery mode cavity, New J. Phys. **12**, 113039 (2010).
[56] S. D. Bennett, N. Y. Yao, J. Otterbach, P. Zoller, P. Rabl, and M. D. Lukin, Phonon-induced spin-spin interactions in diamond nanostructures: application to spin squeezing, Phys. Rev. Lett. **110**, 156402 (2013).
[57] I. Jakobi, S. A. Momenzadeh, F. F. de Oliveira, J. Michl, F. Ziem, M. Schreck, P. Neumann, A. Denisenko, and J. Wrachtrup, Efficient creation of dipolar coupled nitrogen-vacancy spin qubits in diamond, J. Phys.: Conf. Ser. **752**, 012001 (2016).
[58] S. Putz, D. O. Krimer, R. Amsüss, A. Valookaran, T. Nöbauer, J. Schmiedmayer, S. Rotter, and J. Majer, Protecting a spin ensemble against decoherence in the strong-coupling regime of cavity QED, Nat. Phys. **10**, 720 (2014).
[59] D. Kikuchi, D. Prananto, K. Hayashi, A. Laraoui, N. Mizuochi, M. Hatano, E. Saitoh, Y. Kim, C. A. Meriles, and T. An, Long-distance excitation of nitrogen-vacancy centers in diamond via surface spin waves, Appl. Phys. Express **10**, 103004 (2017).
[60] S. B. Zheng and G. C. Guo, Efficient scheme for two-atom entanglement and quantum information processing in cavity QED, Phys. Rev. Lett. **85**, 2392 (2000).
[61] D. F. James and J. Jerke, Effective Hamiltonian theory and its applications in quantum information, Can. J. Phys. **85**, 625 (2007).
[62] T. Holstein and H. Primakoff, Field dependence of the intrinsic domain magnetization of a ferromagnet, Phys. Rev. **58**, 1098 (1940).
[63] K. Hammerer, A. S. Sørensen, and E. S. Polzik, Quantum interface between light and atomic ensembles, Rev. Mod. Phys. **82**, 1041 (2010).
[64] C. P. Yang, Q. P. Su, S. B. Zheng, and S. Han, One-step transfer or exchange of arbitrary multipartite quantum states with a single-qubit coupler, Phys. Rev. B **92**, 054509 (2015).
[65] M. Hofheinz, E. M. Weig, M. Ansmann, R. C. Bialczak, E. Lucero, M. Neeley, A. D. O'Connell, H. Wang, J. M. Martinis, and A. N. Cleland, Generation of Fock states in a superconducting quantum circuit, Nature **454**, 310 (2008).
[66] B. Vlastakis, G. Kirchmair, Z. Leghtas, S. E. Nigg, L. Frunzio, S. M. Girvin, M. Mirrahimi, M. H. Devoret, R. J. Schoelkopf, Deterministically encoding quantum information using 100-Photon Schröinger cat states, Science **342**, 607 (2013).
[67] N. Ofek, A. Petrenko, R. Heeres,P. Reinhold, Z. Leghtas, B. Vlastakis, Y. Liu, L. Frunzio, S. M. Girvin, L. Jiang, M. Mirrahimi, M. H. Devoret, and R. J. Schoelkopf, Extending the lifetime of a quantum bit with error correction in superconducting circuits, Nature **536**, 441 (2016).
[68] R. W. Heeres, P. Reinhold, N. Ofek, L. Frunzio, L. Jiang, M. H. Devoret, and R. J. Schoelkopf, Implementing a universal gate set on a logical qubit encoded in an oscillator, Nat. Commun. **8**, 94 (2017).
[69] U. L. Andersen, J. S. Neergaard-Nielsen, P. van Loock, and A. Furusawa, Hybrid discrete-and continuous-variable quantum information, Nat. Phys. **11**, 713 (2015).
[70] K. Heshami, C. Santori, B. Khanaliloo, C. Healey, V. M. Acosta, P. E. Barclay, and C. Simon, Raman quantum memory based on an ensemble of nitrogen-vacancy centers coupled to a microcavity, Phys. Rev. A **89**, 040301(R) (2014).
[71] H. Bernien, L. Childress, L. Robledo, M. Markham, D. Twitchen, and R. Hanson, Two-photon quantum interference from separate nitrogen vacancy centers in diamond, Phys. Rev. Lett. **108**, 043604 (2012).
[72] C. Santori, D. Fattal, S. M. Spillane, M. Fiorentino, R. G. Beausoleil, A. D. Greentree, P. Olivero, M. Draganski, J. R. Rabeau, P. Reichart, B. C. Gibson, S. Rubanov, D. N. Jamieson, and S. Prawer, Coherent population trapping in diamond N-V centers at zero magnetic field, Opt. Express **14**, 7986 (2006).
[73] C. Santori, P. E. Barclay, K. C. Fu, R. G. Beausoleil, S. Spillane, and M. Fisch, Nanophotonics for quantum optics using nitrogen-vacancy centers in diamond, Nanotechnology **21**, 274008 (2010).
[74] T. Nöbauer, K. Buczak, A. Angerer, S. Putz, G. Steinhauser, J. Akbarzadeh, H. Peterlik, J. Majer, J. Schmiedmayer, and M. Trupke, Creation of ensembles of nitrogen-vacancy centers in diamond by neutron and electron irradiation, arXiv:1309.0453.
[75] K. Sandner, H. Ritsch, R. Amsüss, C. Koller, T. Nöbauer, S. Putz, J. Schmiedmayer, and J. Majer, Strong magnetic coupling of an inhomogeneous nitrogen-vacancy ensemble to a cavity, Phys. Rev. A **85**, 053806 (2012).
[76] C. Santori, P. Tamarat, P. Neumann, J. Wrachtrup, D. Fattal, R. G. Beausoleil, J. Rabeau, P. Olivero, A. D. Greentree, S. Prawer, F. Jelezko, and P. Hemmer, Coherent population trapping of single spins in diamond under optical excitation, Phys. Rev. Lett. **97**, 247401 (2006).
[77] P. Tamarat, N. B. Manson, J. P. Harrison, R. L. McMurtrie, A. Nizovtsev, C. Santori, R. G. Beausoleil, P. Neumann, T. Gaebel, F. Jelezko, P. Hemmer, and J. Wrachtrup, Spin-flip and spin-conserving optical transitions of the nitrogen-vacancy centre in diamond, New. J. Phys. **10**, 045004 (2009).
[78] Z. L. Xiang, S. Ashhab, J. Q. You, and F. Nori, Hybrid quantum circuits: Superconducting circuits interacting with other quantum systems, Rev. Mod. Phys. **85**, 623 (2013).

[79] A. A. Savchenkov, A. B. Matsko, V. S. Ilchenko, and L. Maleki, Optical resonators with ten million finesse, Opt. Express **15**, 6768 (2007).

[80] V. Huet, A. Rasoloniaina, P. Guillemé, P. Rochard, P. Fron, M. Mortier, A. Levenson, K. Bencheikh, A. Yacomotti, and Y. Dumeige, millisecond photon lifetime in a slow-light microcavity, Phys. Rev. Lett. **116**, 133902 (2016).

[81] A. Megrant, C. Neill, R. Barends, B. Chiaro, Y. Chen, L. Feigl, J. Kelly, E. Lucero, M. Mariantoni, P. J. J. O'Malley, D. Sank, A. Vainsencher, J. Wenner, T. C. White, Y. Yin, J. Zhao, C. J. Palmstrøm, J. M. Martinis, and A. N. Cleland, Planar superconducting resonators with internal quality factors above one million, Appl. Phys. Lett. **100**, 113510 (2012).

[82] P. L. Stanwix, L. M. Pham, J. R. Maze, D. Le Sage, T. K. Yeung, P. Cappellaro, P. R. Hemmer, A. Yacoby, M. D. Lukin, and R. L. Walsworth, Coherence of nitrogen-vacancy electronic spin ensembles in diamond, Phys. Rev. B **82**, 201201(R) (2010).

[83] P. C. Maurer, G. Kucsko, C. Latta, L. Jiang, N. Y. Yao, S. D. Bennett, F. Pastawski, D. Hunger, N. Chisholm, M. Markham, D. J. Twitchen, J. I. Cirac, and M. D. Lukin, Room-temperature quantum bit memory exceeding one second, Science **336**, 1283 (2012).

[84] E. D. Herbschleb, H. Kato, Y. Maruyama, T. Danjo, T. Makino, S. Yamasaki, I. Ohki, K. Hayashi, H. Morishita, M. Fujiwara, and N. Mizuochi, Ultra-long coherence times amongst room-temperature solid-state spins, Nat. Commun. **10**, 3766 (2019).

[85] E. Neu, C. Hepp, M. Hauschild, S. Gsell, M. Fischer, H. Sternschulte, D. S. Nethl, M. Schreck, and C. Becher, Low-temperature investigations of single silicon vacancy colour centres in diamond, New J. Phys. **15**, 043005 (2013).

[86] D. D. Sukachev, A. Sipahigil, C. T. Nguyen, M. K. Bhaskar, R. E. Evans, F. Jelezko, and M. D. Lukin, Silicon-vacancy spin qubit in diamond: a quantum memory exceeding 10 ms with single-shot state readout, Phys. Rev. Lett. **119**, 223602 (2017).

[87] C. Weinzetl, J. Görlitz, J. N. Becker, I. A. Walmsley, E. Poem, J. Nunn, and C. Becher, Coherent control and wave mixing in an ensemble of silicon-vacancy centers in diamond, Phys. Rev. Lett. **122**, 063601 (2019).

[88] M. Widmann, S. Y. Lee, T. Rendler, N. T. Son, H. Fedder, S. Paik, L. P. Yang, N. Zhao, S. Yang, I. Booker, A. Denisenko, M. Jamali, S. A. Momenzadeh, I. Gerhardt, T. Ohshima, A. Gali, E. Janzén, and J. Wrachtrup, Coherent control of single spins in silicon carbide at room temperature, Nature Materials **14**, 164 (2015).

[89] S. G. Carter, Ö. O. Soykal, P. Dev, S. E. Economou, and E. R. Glaser, Spin coherence and echo modulation of the silicon vacancy in 4H-SiC at room temperature, Phys. Rev. B **92**, 161202(R) (2015).

[90] W. F. Koehl, B. B. Buckley, F. J. Heremans, G. Calusine, and D. D. Awschalom, Room temperature coherent control of defect spin qubits in silicon carbide, Nature **479**, 84 (2011).

[91] D. J. Christle, A. L. Falk, P. Andrich, P. V. Klimov, J. U. Hassan, N. T. Son, Erik Janzén, T. Ohshima, and D. D. Awschalom, Isolated electron spins in silicon carbide with millisecond coherence times, Nature Materials **14**, 160 (2015).